V. NUCLEAR MAGNETIC RESONANCE AND HYPERFINE STRUCTURE

Prof. F. Bitter	B. B. Aubrey	R. H. Kohler
Prof. L. C. Bradley III	M. Çiftan	R. F. Lacey
Prof. J. S. Waugh	F. W. Dobbs	J. H. Loehlin
Dr. S. P. Davis	R. W. Fessenden	I. G. McWilliams
Dr. P. L. Sagalyn	H. R. Hirsch	A. C. Melissinos
Dr. H. H. Stroke	R. J. Hull	S. T. Wray, Jr.

RESEARCH OBJECTIVES

1. Nuclear Magnetic Resonance

(a) Nuclear Spin Interactions in Molecules. It has become clear that high-resolution nuclear-resonance experiments can give a great deal of information relative to the geometrical and electronic structures of molecules. It is believed that all observed spectral structures can be accounted for on the basis of the Hamiltonian

$$\frac{1}{\hbar}\mathscr{H} = H \sum_i \gamma_i(1 - \delta_i) + \sum_i \sum_{j>i} J_{ij}\, \vec{I}_i \cdot \vec{I}_j$$

where H is the applied magnetic field, γ_i is the gyromagnetic ratio of nucleus i, $\vec{I}_i$ is its spin operator, and δ_i and J_{ij} are coupling constants characteristic of the electronic wavefunctions of the molecule. We are attempting to justify the form of this Hamiltonian in intermediate coupling cases, and to correlate the coupling constants with simple descriptions of the molecular wavefunctions. Standard radiofrequency techniques are being used, with particular attention to the magnetic field uniformity and stability which will permit resolution of lines separated by approximately 1 part in 10^8 of the total field.

(b) Molecular Motion in Solids. Large-scale motion in solids can have important effects on the macroscopic properties of substances in which they occur. This fact is particularly evident in solid-state diffusion and chain twisting in polymers such as rubber. Nuclear-resonance linewidth measurements can give rather direct information on the types of motion that are present and on their activation energies. We are applying this method to cases that are not practicably accessible by other methods, with special reference to ion and terminal group reorientation. Results which have been obtained deal with $Co(NH_3)_6^{+++}$ and MF_6^- ions and $-CH_3$ and $-CF_3$ groups in various crystal lattices.

J. S. Waugh

2. Hyperfine Structure

The purpose of this work is to learn about nuclear structure from detailed investigations of atomic energy levels. Atomic electrons actually penetrate the nucleus in the course of their orbital motion, and the position of the various possible energy levels is influenced by the electron-nuclear interaction.

The investigations of this group are concerned with changes in the energy levels produced by reorientation of the nucleus with respect to the atomic angular momentum, and with accurate comparison of energy levels of isotopes, both stable and unstable. A combination of radiofrequency or microwave and optical techniques is being used.

Previously reported investigations of the isotopes of mercury are being extended.

F. Bitter, L. C. Bradley III

(V. NUCLEAR MAGNETIC RESONANCE)

A. ATOMIC-BEAM LIGHT SOURCES

Calculations have been made on the emission (or absorption) of light that is to be expected from an atomic beam. The calculations were made for a particular beam geometry: two similar rectangular slits, with dimensions Δy and Δz, are placed a distance A apart (see Fig. V-1). In the oven are atoms that are assumed to have a Maxwellian velocity distribution, with a density sufficiently low that collisions near the first slit and in the beam itself can be neglected. The beam is considered as being viewed from a direction approximately perpendicular to the side Δz, and sufficient collimation is assumed so that $\alpha \equiv (\Delta y/A) \ll 1$.

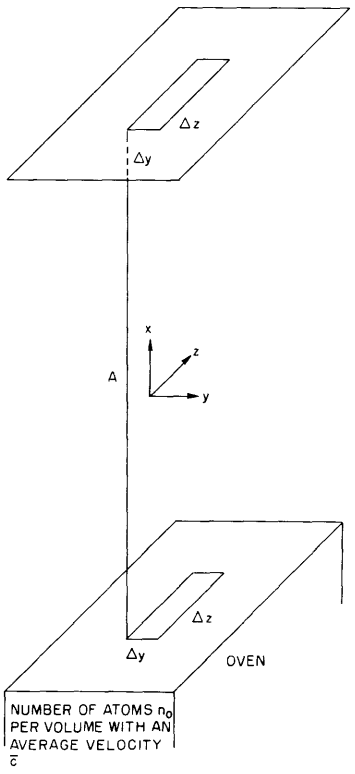

Fig. V-1. Schematic drawing of the beam configuration for which calculations were made.

The light emitted (or absorbed) by such a beam will be broadened chiefly by the Doppler effect, and by natural broadening; for practical collimations, the Doppler effect will usually predominate. The Doppler shift $\Delta\nu_D$, in a line of frequency ν_o emitted (or absorbed) by an atom, is $(\Delta\nu_D)/\nu_o = v_s/c$, where v_s is the velocity of the atom in the line of sight. We wish to calculate $n(v_s)$, the number of atoms in the beam with a given velocity in the line of sight, which is not necessarily exactly perpendicular to the beam axis, although in practical cases it will be nearly so. We also want to learn the effect of using a finite cone of light from the beam, as collected by a lens, for example.

It is convenient to use dimensionless velocity components

$$u^2 = \frac{m}{2kT} v_x^2, \quad v^2 = \frac{m}{2kT} v_y^2, \quad w^2 = \frac{m}{2kT} v_z^2, \quad s^2 = \frac{m}{2kT} v_s^2$$

where T is the temperature in the oven. In our approximation, $s = v + u\theta \cos\phi$, where θ and ϕ are polar angles referred to the y-axis, and we have assumed that $\sin\theta \approx \theta$ and $w \ll u$. (The last is our most dubious assumption; its validity will depend on the ratio $\Delta z/A$.)

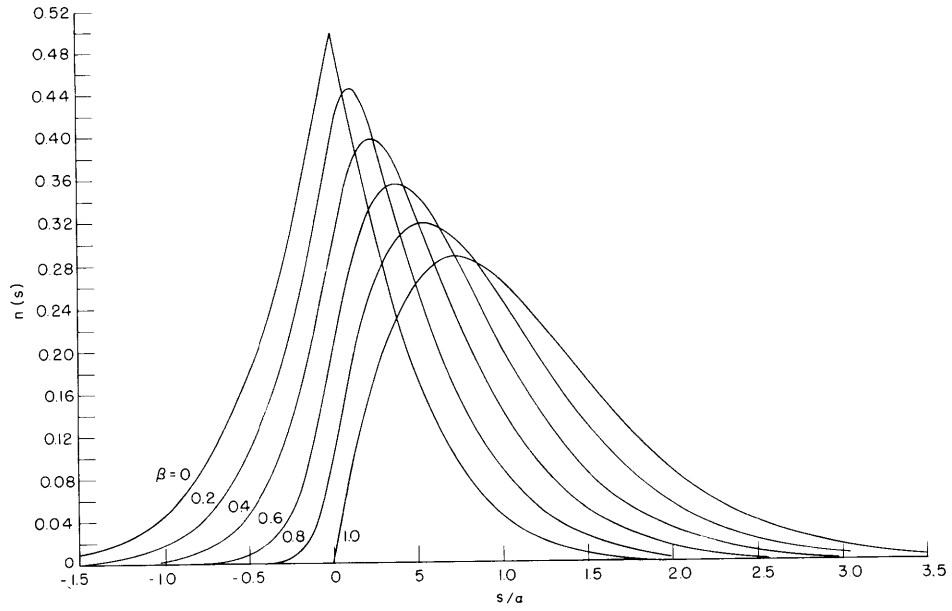

Fig. V-2. Number of atoms n(s) with a given velocity, $v_s = s\sqrt{\frac{2kT}{m}}$, in the line of sight, plotted as a function of $\frac{s}{a}$, for different values of the parameter $\beta = \frac{\theta \cos \phi}{a}$.

Figure V-2 shows plots of n(s) as a function of s/a, for several values of the parameter $\beta \equiv (\theta \cos \phi)/a$ between zero and unity. An increased value of β leads to a shift in the maximum, and to a broadening of the curve, as might be expected. The shift of the maximum is almost linear for $\beta \leq 0.4$, but departs from linearity for larger angles.

Figure V-3 shows the Doppler shape of the light collected by a lens of finite size which collects all of the light that is emitted in a cone of half-angle γa. The intensity distribution is plotted as a function of s/a for values of the parameter $\gamma = 0.3, 0.7, 1.0$; only positive values of s/a are shown, since the distribution is symmetrical about the origin. The most curious feature of these curves is the fact that there are two maxima symmetrically placed about the origin. This can be understood if one imagines that the lens is cut in half; the upper half will produce a line with a displaced maximum, the lower half will produce a line with a shape that is the mirror image, and the two maxima will not necessarily merge to form a single maximum.

Another interesting point in Fig. V-3 is the line breadth. This quantity can be defined in various ways, and it is hard to compare breadths when the shape of the line varies. Qualitatively, though, it can be seen that $\gamma = 0.3$ and $\gamma = 0.7$ give nearly the same breadth, perhaps 30 per cent larger than that for $\gamma = 0$; but, since the total intensity is proportional to γ^2, it will usually be profitable to work at $\gamma \approx 0.7$. For $\gamma = 1.0$, however,

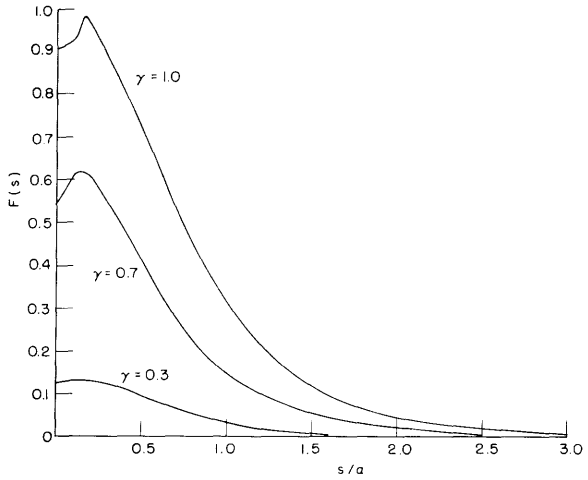

Fig. V-3. Doppler broadening of a spectral line, emitted or absorbed by the beam and collected by a lens subtending a half-angle γa. The integrated intensity F(s) is plotted on an arbitrary scale against $\frac{s}{a} = \frac{c}{a}\sqrt{\frac{m}{2kT}}\,\frac{\Delta\nu_D}{\nu_o}$, where $\Delta\nu_D$ is the Doppler shift corresponding to the velocity s in the line of sight.

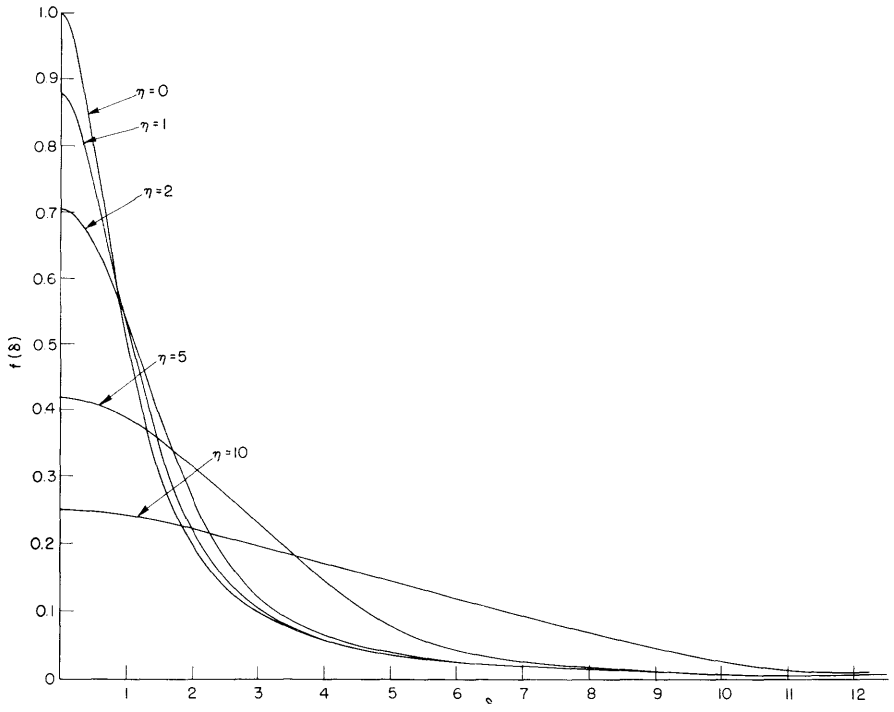

Fig. V-4. Shape of a line broadened by both natural broadening and the Doppler effect. The intensity (in arbitrary units) is plotted against $\delta = \frac{\nu - \nu_o}{\epsilon/2}$, where ϵ is the natural linewidth at half-maximum.

the extra broadening is appreciable.

In our calculations the natural broadening has been neglected. It will always be more important than the Doppler effect at large distances from the center of the line. The actual line shape when Doppler and natural broadening have comparable widths is shown in Fig. V-4, for $\beta = 0$ and for several values of the parameter $\eta \equiv 2/\epsilon \cdot (a\nu_o/c)\,[(kT)/m]^{1/2}$, where ϵ is the natural line width at half-maximum, and T is the temperature in the oven, so that η is essentially a measure of the ratio of Doppler width to natural width. The intensity is shown as a function of $\delta \equiv (\nu - \nu_o)/(\epsilon/2)$. Calculations have not been made for $\beta \neq 0$.

The other significant quantity is the number of atoms per unit area in the beam; this number is $(n_o/4\pi)\, a^2\, \Delta z$, where n_o is the atom density in the oven. This density may be increased until the mean free path in the oven is Δy, or $n_o = (\sigma \Delta y)^{-1}$, where σ is the collision cross section.

F. Bitter, L. C. Bradley III

B. HYPERFINE STRUCTURE OF THE P STATE OF MERCURY BY DOUBLE-RESONANCE METHODS

1. In Zero Magnetic Field

The transition, F = 3/2 to F = 1/2, ^3P, in Hg^{201} has been observed in zero magnetic field by a method that was proposed in the Quarterly Progress Report of July 15, 1956, page 20. The following modifications have been introduced:

1. The resonance cell filled with natural-mercury vapor is replaced by a cell filled with Hg^{201}.
2. The waveguide is replaced by a tunable cavity.
3. Photomultiplier II and the quartz plate are omitted.

The random-drift problem has been solved by modulating the microwave intensity at 30 cps. Near the ΔF resonant frequency there is partial 30-cycle modulation of the intensity of the light that enters photomultipler I, and its output current, therefore, contains a 30-cycle component, which is easily extracted by an electric filter network.

R. H. Kohler